Available online at www.sciencedirect.com
ScienceDirect
Trans. Nonferrous Met. Soc. China 23(2013) 400−405
Transactions of Nonferrous Metals Society of China
www.tnmsc.cn

Sliding wear behavior of magnetorheological fluid for brass with and without magnetic field

Wan-Li SONG, Chul-Hee LEE, Seung-Bok CHOI

Department of Mechanical Engineering, Inha University, Incheon 402-751, Korea

Received 2 May 2012; accepted 30 October 2012

Abstract: A pin-on-disc wear apparatus was used to carry out the tribological experiment of brass to investigate the effect of a magnetorheological (MR) fluid on the interfacial surface with and without magnetic field. A series of tests were performed at the loads of 20−100 N and rotating speeds of 127−425 r/min for 2 h. The friction coefficient and wear rate were monitored by the wear apparatus, while the microstructures of the worn surfaces were observed by scanning electron microscope (SEM). In addition, the chemical composition of worn surfaces was analyzed by energy dispersive X-ray spectroscopy (EDS). Test results show different friction and wear performance of the MR fluid with and without magnetic field. At the same time, the effects of various normal loads and rotating speeds on the tribological behavior were investigated. Through the investigation of the morphologies of the worn surfaces under the magnetic field, it is found that the MR particles are clearly evident on the worn surface and the plastic flow of ridges causes the lateral extrusion. This directly indicates that abrasive wear is the predominant wear mechanism observed with MR fluid.

Key words: magnetorheological fluid; sliding wear; brass; magnetic field; friction coefficient

1 Introduction

In recent years, magnetorheological (MR) and electrorheological (ER) fluids have been received a great attention because of the transformation of their rheological properties, and numerous studies have been performed to enhance the dielectric properties and MR/ER effect [1−3]. Thereby, developments of MR/ER fluids in many applications, such as polishing technology and dampers, have become more extensive in the past few years [4−6]. Furthermore, it has been proved that the MR fluid has better advantages than the ER fluid, such as control effect, operational field, stability and operational temperature. All of these technology advantages of MR fluids have created a very high level of interest to introduce new products [7].

However, MR fluids also have a serious drawback to restrict the applications of MR fluids. For example, MR fluid leads to high friction and wear, galling and seizing for contacting parts. Up till now, there have been some studies of the friction and wear properties of MR/ER fluids. WONG et al [8,9] investigated the tribological behavior of an MR fluid in the unexcited mode of operation under boundary lubrication conditions using a block-on-ring tester. This research indicated that the MR fluid could perform better than the ER fluid in the absence of magnetic field under boundary lubrication conditions. And it has been found that the particle bunching and apparent surface changed along with the iron concentration of MR fluid were put forward. SOHN et al [10] investigated the wear characteristics of the MR fluid under boundary lubrication contact conditions. SEOK et al [11] examined the tribological properties of the MR fluid in a finishing process. The experimental results showed that the dominant wear mechanism during a finishing process was abrasion, and a semi-empirical material removal model was proposed for the description of the tribological behavior of MR fluid. LINGARD et al [12] studied the wear performance and boundary lubrication properties of a silicone-oil-based ER fluid on a two-disc machine. It was concluded that the ER fluid was likely to cause severe wear problems in some engineering situations.

CHOI et al [13] researched the wear characteristics of a phosphorated starch-based ER fluid without an

Foundation item: Project (2010-0015090) supported by the National Research Foundation of Korea
Corresponding author: Seung-Bok CHOI; Tel: +82-32-8607319; E-mail: seungbok@inha.ac.kr
DOI: 10.1016/S1003-6326(13)62476-0

electric field. The results showed that the ER fluid with the phosphorated starch particles had the stabilized wear and friction characteristics, but the wear rate was increased compared with the case of only silicone oil.

Most of the above investigations were applied to MR/ER fluids in the absence of external field, even though the most prominent advantage of MR/ER fluids is transformation of rheological property under the external field. In addition, steel was studied as a main material in the above mentioned studies. But, brass is also one of the materials which are extensively used in the parts of machines. Brass has an attractive combination of the properties, namely, good corrosion resistance, good wear properties, and high thermal and electrical conductivity [14−16].

Consequently, the goal of this study is to investigate the sliding wear characteristics of MR fluid with and without magnetic field for brass specimens. The sliding wear experiments were carried out to evaluate the variation of the friction coefficient and wear rate of brass specimens lubricated by MR fluid with and without magnetic field. In addition, the effects of different normal loads and rotating speeds on the wear performance were investigated.

2 Experimental

A pin-on-disc apparatus was used to carry out the tribological experiment of brass to investigate the effect of MR fluid on the interfacial surface of the brass specimen with and without a magnetic field. Figure 1 shows the schematic drawing of the pin-on-disc device. The disc is located in the electromagnet, and the contacting interface is immersed in the MR fluid. The MR fluid used in the tests was Lord MRF−132DG fluid which is a suspension of micron-sized, magnetizable particles in a carrier fluid. The viscosity at 40 °C, particle size, density, volume fraction of MR particles and operating temperature of the MR fluid are shown in Table 1. A photograph of the typical specimen is shown in Fig. 2. The pin had a diameter of 5 mm and a length of 30 mm, and the disk had the diameter and thickness of 60 mm and 10 mm, respectively. A series of tests were

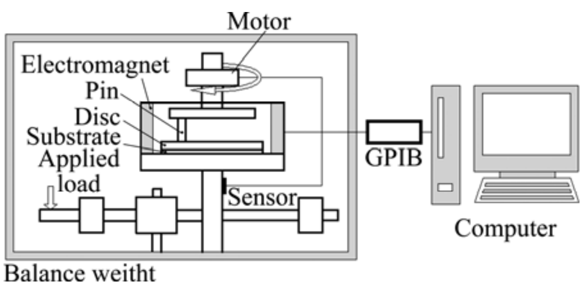

Fig. 1 Schematic drawing of pin-on-disc device

Table 1 Properties of MR fluid

Variable	Value
Viscosity (40°C)/(Pa·s)	0.092±0.015
Particle size/μm	1−4
Density/(g·cm^{-3})	2.98−3.18
Volume fraction of MR particle/%	32
Operating temperature/°C	−40−130
Humidity/%	40−50

Fig. 2 Photograph of pin and disc

performed at the load of 20−100 N, rotating speed of 127−425 r/min, 2 h duration time and 20−25 °C temperature. The magnetic induction applied was 5×10^{-4} T in this experiment.

In this work, the variations of the wear rate and friction coefficient were studied under lubricating by MR fluid with and without magnetic field. The wear rate was calculated as follows:

$$I=\frac{\mathrm{d}l}{\mathrm{d}t} \tag{1}$$

where I is the wear rate, dl is the length of pin loss, and dt is the sliding time. Then, the friction coefficient was calculated by

$$\mu=\frac{T}{Nr} \tag{2}$$

where T is torque measured by torque sensor, N is the normal load, and r is the track radius of pin specimen.

The specimens were cleaned with alcohol and acetone after each test. The microstructures of the worn surfaces were observed by scanning electron microscope (SEM) and the chemical composition of worn surfaces was analyzed by energy dispersive X-ray spectroscopy (EDS). The surface roughness profiles of the discs were also determined by the profilemeter before and after the wear test.

3 Results and discussion

Figure 3 shows the wear rate and friction coefficient of brass with and without magnetic field at normal load of 50 N and rotating speed of 297 r/min. As can be seen in Fig. 3(a), the wear rate at 5×10^{-4} T increases sharply until 60 min and then gets a steady state, while the wear rate without magnetic field increases steadily. Although the wear rate with magnetic field is higher than that without magnetic field at the initial phase, it gets into the almost same value at the end of test. This indicates that the magnetic field has a negative effect on wear rate at the initial wear stage; this is believed to be caused by the agglomeration of iron particles. It is well known that the MR particles are easy to aggregate under the magnetic field and brass is nonmagnetic metal. The aggregation of MR particles is not asymmetrical because there are not magnetic forces of particles and specimen surface. Thus, the asymmetrical agglomeration aggravates the wear of the specimen surface, especially at the initial wear stage. As the wear process goes on, the effect of the micron-sized MR particles on wear becomes insignificant compared with the harsh worn surface, and it is quite likely that the particles play a role in the compensation of wear. Thus, the wear rate becomes relatively steady during the later stage. However, the friction coefficient without magnetic field exhibits an increasing trend in the wear process while the friction coefficient with a magnetic field exhibits a steady trend as shown in Fig. 3(b).

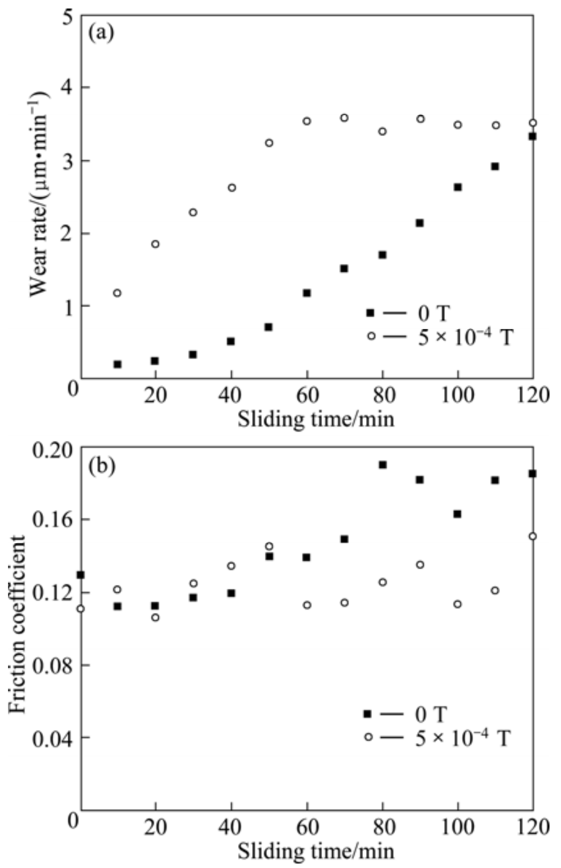

Fig. 3 Wear rate (a) and friction coefficient (b) with and without magnetic field

The wear rate and friction coefficient of brass specimen at 5×10^{-4} T under different normal loads (20−100 N) are presented in Fig. 4. It is observed in Fig. 4(a) that the wear rate increases with increasing the normal load. Moreover, the slope of wear rate versus sliding time increases with increasing the normal load. The factors responsible for low wear are that copper readily oxidizes in air so that there is a little metallic contact at low loads. However, the oxide film breaks down easily, resulting in intimate metallic contact, which is responsible for high wear and surface damage. As shown in Fig. 4(b), the friction coefficient exhibits a decreasing trend with increasing normal load. Compared with the curves in Fig. 3, the slopes of wear rate in Fig. 4(a) are small at the later stage and all the curves in Fig. 4(b) present a stable behavior owing to the effect of magnetic field.

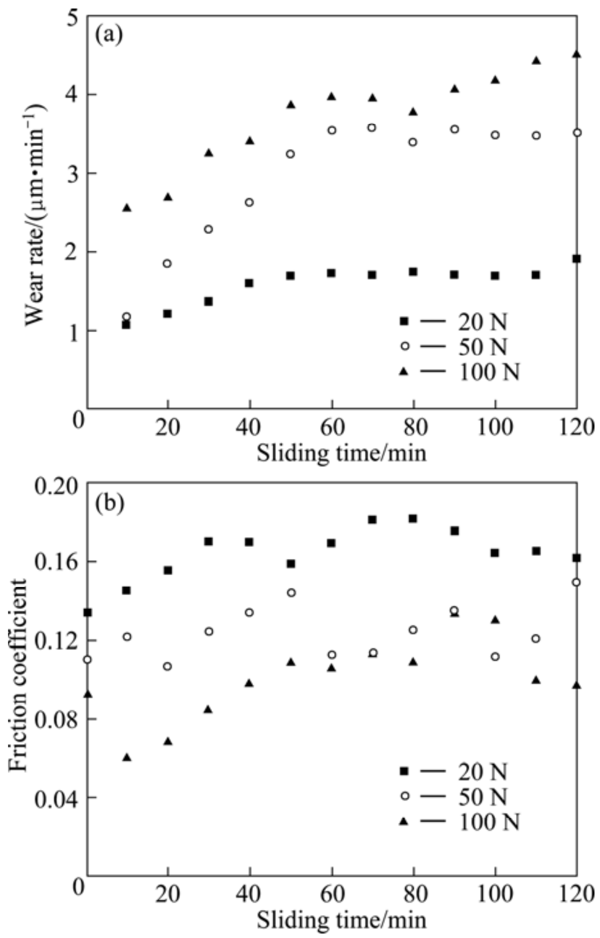

Fig. 4 Wear rate (a) and friction coefficient (b) with time under different normal loads

Figure 5 shows the wear rate and friction coefficient at 50 N and 5×10^{-4} T under various rotating speeds. The wear rate increases with increasing the rotating speed, and the wear rate at 297 or 425 r/min is evidently higher than that at 127 r/min. This is responsible for the increase of sliding distance because of its low rotating speed. Moreover, for the speeds of 297 and 425 r/min, the wear rates are almost same. This means that more MR particles are trapped onto the contact surfaces and separate the two contact surfaces at high speeds, resulting in the decrease of wear. In Fig. 5(b), the friction coefficient is extremely irregular along with sliding time at various rotating speeds, and the friction coefficients are in the range from 0.08 to 0.16.

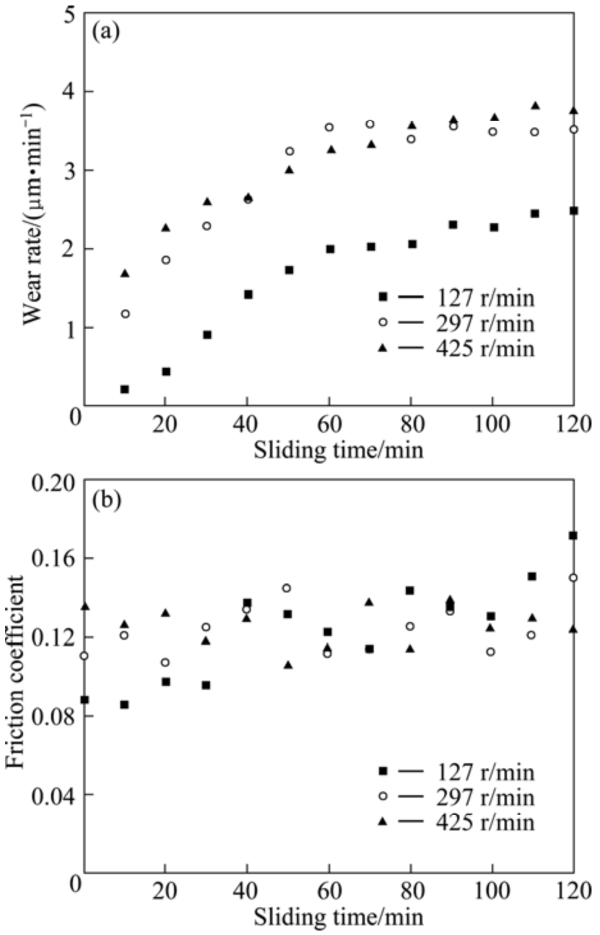

Fig. 5 Wear rate (a) and friction coefficient (b) with time under various rotating speeds

Figure 6 shows the topography of the brass disc before and after the test by SEM. The test conditions are the normal load of 100 N and rotating speed of 297 r/min at 5×10^{-4} T of magnetic induction. The original machining marks in Fig.6 (a) are completely missing across the worn surface of the brass disc; instead, there is an evidence of many sliding lines and more grooves on the wear track in Fig. 6(b). It should be remarkable that a lump of particles can be seen partly embedded on the worn surface and the plastic flow of the ridges causes lateral extrusion. This indicates that the MR particles and wear debris act as the abrasive material and the predominant type of wear is abrasive wear.

The chemical composition of the pin surfaces before and after tests is summarized in Table 2. Figure 7 displays the EDS spectra of the brass pin before and after tests. The test conditions are the normal load of 100 N and rotating speed of 297 r/min at 5×10^{-4} T. Observing the difference of chemical composition of the original and worn surface, there is an evidence of the existence of Fe element on the worn surface, which indicates that material transfers from the MR particles to the pin.

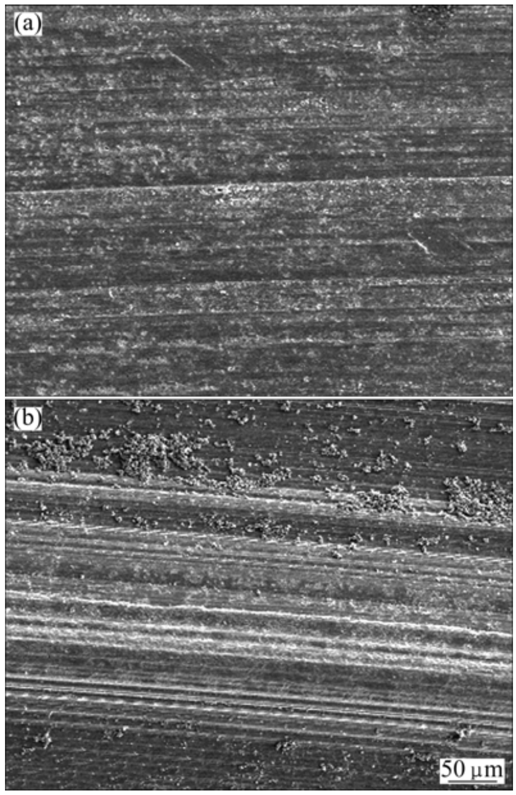

Fig. 6 SEM morphologies of initial surface (a) and worn surface (b) of disc

Table 2 Chemical composition of pin surfaces before and after experiment

Sample	w(C)/%	w(O)/%	w(Fe)/%	w(Cu)/%	w(Zn)/%
Original pin	8.06	2.51	−	49.68	39.75
Worn pin	10.67	3.51	1.01	47.74	37.07

The resulting depth of wear trace was presented by detecting the surface profiles of the original and worn specimen in Fig. 8. The applied normal load, rotating speed and magnetic induction are 100 N, 297 r/min and 5×10^{-4} T, respectively. In Fig. 8(b), there is an obvious sunken wear trace in the middle of the measured area after the wear test compared with the original surface profile in Fig. 8(a). The initial average surface roughness (R_a) is 1.0458 μm before the wear test and the surface roughness is 7.5716 μm after the wear test. This indicates that the wear surface due to the MR particles under boundary condition is very harsh (determined in Fig. 6(b)).

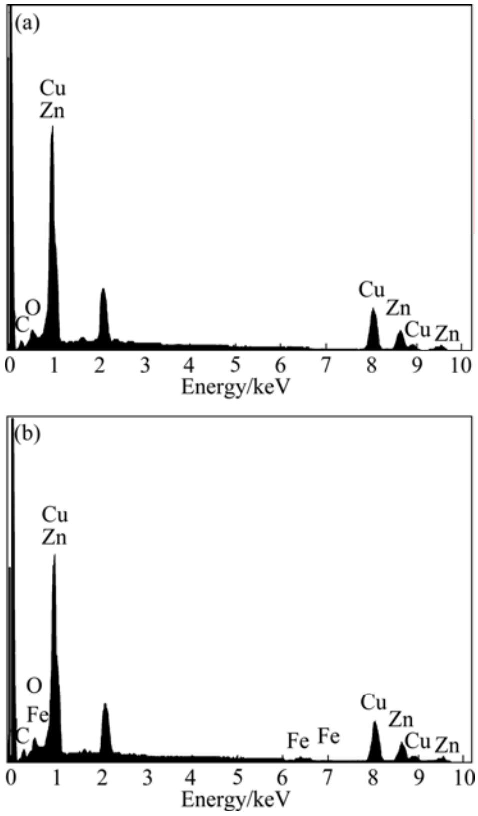

Fig. 7 EDS spectra of initial surface (a) and worn surface (b) of pin

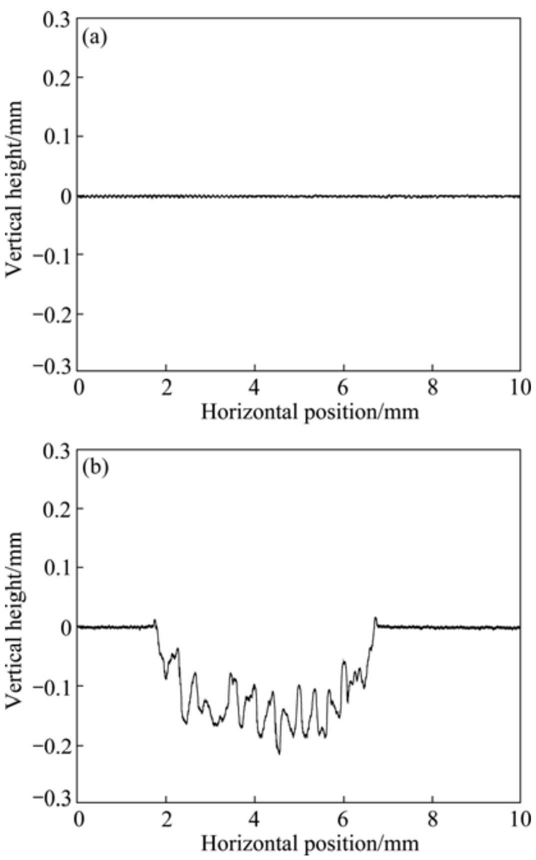

Fig. 8 Measured surface profiles of traces before (a) and after (b) wear test

4 Conclusions

The wear rate with the magnetic field is higher than that without the magnetic field due to the magnetization of iron particles in the initial phase, and then it gets a relatively steady state. The wear rate is in proportion to the rotating speed and normal load. Through the observation of the worn surfaces by SEM and EDS, it is found that MR particles are trapped onto the counter-surface and the predominant types of the wear is abrasive wear.

References

[1] FURST E M, GAST A P. Micromechanics in magnetorheological suspensions [J]. Physical Review E, 2000, 61: 6732−6739.

[2] LIU Y D, FANG F F, CHOI H J. Silica nanoparticle decorated polyaniline nanofiber and its electrorheological response [J]. Soft Matter, 2011, 7: 2782−2789.

[3] LIU Y D, FANG F F, CHOI H J. Core-shell structured semiconducting PMMA/polyaniline snowman-like anisotropic microparticles and their electrorheology [J]. Langmuir, 2010, 26(15): 12849−12854.

[4] SONG W L, CHOI S B, LEE D W, LEE C H. Micro-precision surface finishing using magneto-rheological fluid [J]. Science China: Technological Sciences, 2012, 55(1): 56−61.

[5] DONG Xiao-min, YU Miao, LIAO Chang-rong, CHEN Wei-min. A new variable stiffness absorber based on magneto-rheological elastomer [J]. Transactions of Nonferrous Metals Society of China, 2009, 19(s3): 611−615.

[6] SUNG K G, CHOI S B, PARK M K. Geometry optimization of magneto-rheological damper for vehicle suspension via finite element method [J]. Advanced Science Letters, 2011, 4(3): 805−809.

[7] OLABI A G, GRUNWALD A. Design and application of magneto-rheological fluid [J]. Materials & Design, 2007, 28(10): 2658−2664.

[8] WONG P L, BULLOUGH W A, FENG C, LINGARD S. Tribological performance of a magneto-rheological suspension [J]. Wear, 2001, 247(1): 33−40.

[9] LEUNG W C, BULLOUGH W A, WONG P L, FENG C. The effect of particle concentration in a magneto-rheological suspension on the performance of a boundary lubricated contact [J]. Proceedings of the Institution of Mechanical Engineers, Part J: Journal of Engineering Tribology, 2004, 218(4): 251−264.

[10] SOHN J W, CHOI S B, LEE C H, CHO M W. Wear characteristics of magnetorheological fluid under boundary lubrication [J]. Advanced Materials Research, 2009, 79−82: 83−86.

[11] SEOK J W, LEE S O, JANG K I, MIN B K, LEE S J. Tribological properties of a magnetorheological (MR) fluid in a finishing process [J]. Tribology Transactions, 2009, 52(4): 460−469.

[12] LINGARD S, BULLOUGH W A, SHEK W M. Tribological performance of an electro-rheological fluid [J]. Journal of Physics D: Applied Physics, 1989, 22(11): 1639−1645.

[13] CHOI S B, SOHN J W, HAN Y M, LEE C H. Wear characteristics under boundary lubrication contacts in phosphorated starch-based electrorheological fluid [J]. Tribology Transactions, 2010, 53(2): 256−265.

[14] EMGE A, KARTHIKEYAN S, KIM H J, RIGNEY D A. The effect of sliding velocity on the tribological behavior of copper [J]. Wear, 2007, 263(1−6): 614−618.
[15] CHEN Zhen-xing, WANG Ling-sen, HUANG Bai-yun. Growth of brass nanofilms sputtered on organic substrate [J]. Transactions of Nonferrous Metals Society of China, 2005, 15(3): 661−665.
[16] GARCÍA P, RIVERA S, PALACIOS M, BELZUNCE J. Comparative study of the parameters influencing the machinability of leaded brasses [J]. Engineering Failure Analysis, 2010, 17(4): 771−776.

在磁场条件下黄铜的磁流变液滑动磨损行为

Wan-Li SONG, Chul-Hee LEE, Seung-Bok CHOI

Department of Mechanical Engineering, Inha University, Incheon 402-751, Korea

摘　要：采用盘销式摩擦磨损装置进行铜摩擦试验，研究在有、无磁场条件下磁流变液对界面表面的影响。在载荷为 20~100 N，转速为 127~425 r/min 下旋转 2 h，进行一系列试验。摩擦因数和磨损率由磨损装置控制，采用扫描电子显微镜(SEM)观察磨损表面的微观组织。此外，采用 X 射线光谱(EDS)分析磨损表面的化学成分。结果显示，在有、无磁场条件下出现了不同的摩擦磨损系数和性能。同时，研究了载荷和转速对摩擦行为的影响。研究了在有磁场条件下的磨损表面形貌，发现在磨损表面明显存在磁流变颗粒，且脊塑流引起了侧向挤出，这表明磨料磨损是磁流变液的主要磨损机制。

关键词：磁流变液；滑动磨损；黄铜；磁场；摩擦因数

(Edited by Xiang-qun LI)